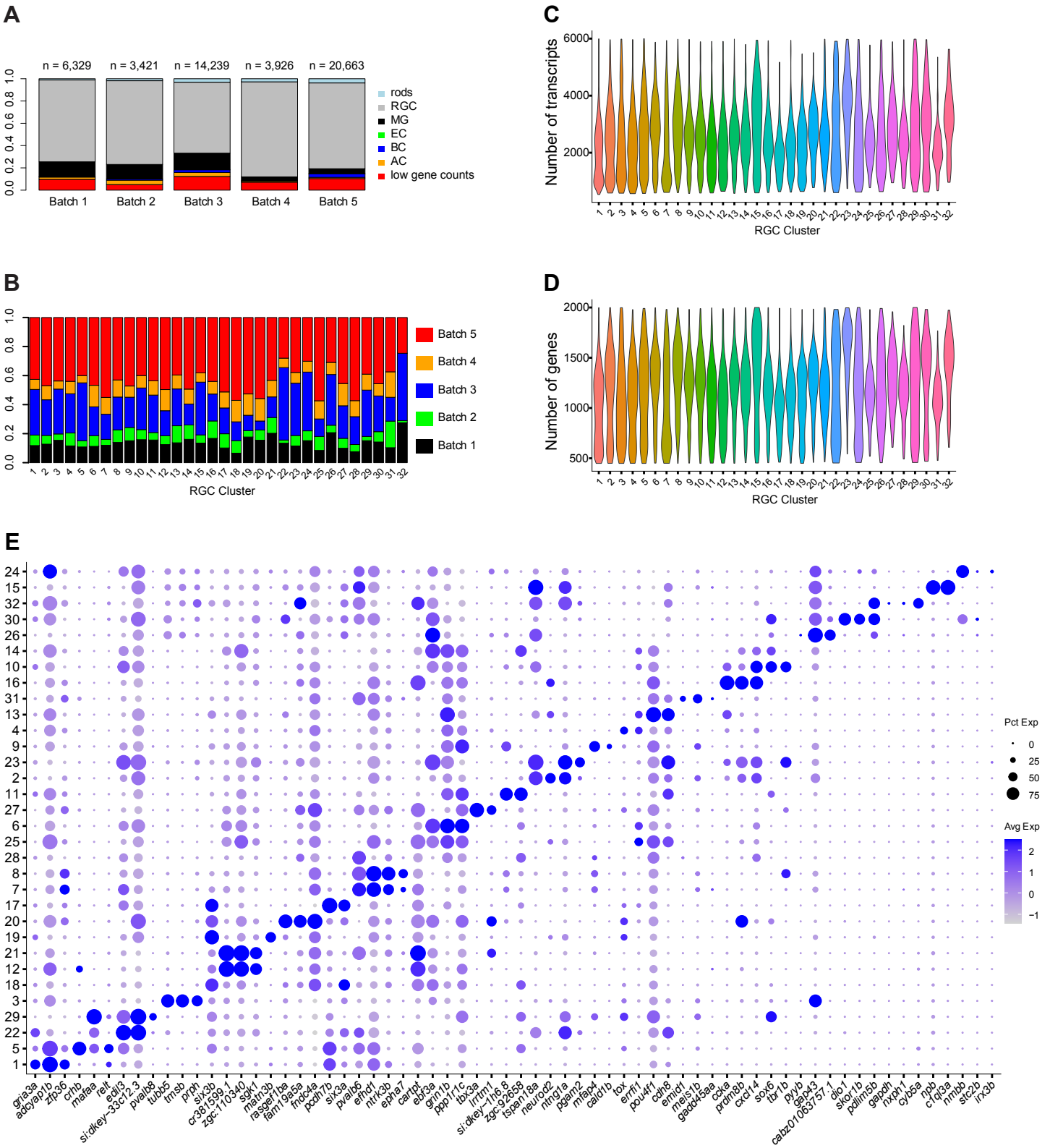
A
n = 6,329
n = 3,421
n = 14,239
n = 3,926
n = 20,663
Batch 1
Batch 2
Batch 3
Batch 4
Batch 5
rods
RGC
MG
EC
BC
AC
low gene counts
B
RGC Cluster
Batch 5
Batch 4
Batch 3
Batch 2
Batch 1
C
Number of transcripts
RGC Cluster
D
Number of genes
RGC Cluster
E
Pct Exp
Avg Exp

Figure S1. Molecular catalog of adult RGCs, related to Figure 1

(A) Barplot showing relative proportions (y-axis) of RGCs, non-RGCs and low-quality cells (colors) in scRNA-seq biological replicates from adult fish (x-axis). Recovered cell numbers from each replicate are indicated on top. non-RGCs include rods, bipolar cells (BC), amacrine cells (AC), Muller glia (MG), and endothelial cells (EC). Clusters containing “cells” with low gene counts that did not exhibit any distinguishing markers were excluded from the analysis.

(B) Barplot showing the relative proportion (y-axis) of each biological replicate in adult RGC clusters (x-axis), showing lack of strong batch effects.

(C) Violin plot showing distributions of the number of transcripts detected per cell (y-axis) in each adult RGC cluster (x-axis).

(D) Violin plot showing distributions of the number of genes detected per cell (y-axis) in each adult RGC cluster (x-axis).

(E) Dotplot showing top three selectively enriched markers (columns) in each adult RGC cluster (rows). Representation and row ordering as in **Figure 1F**.

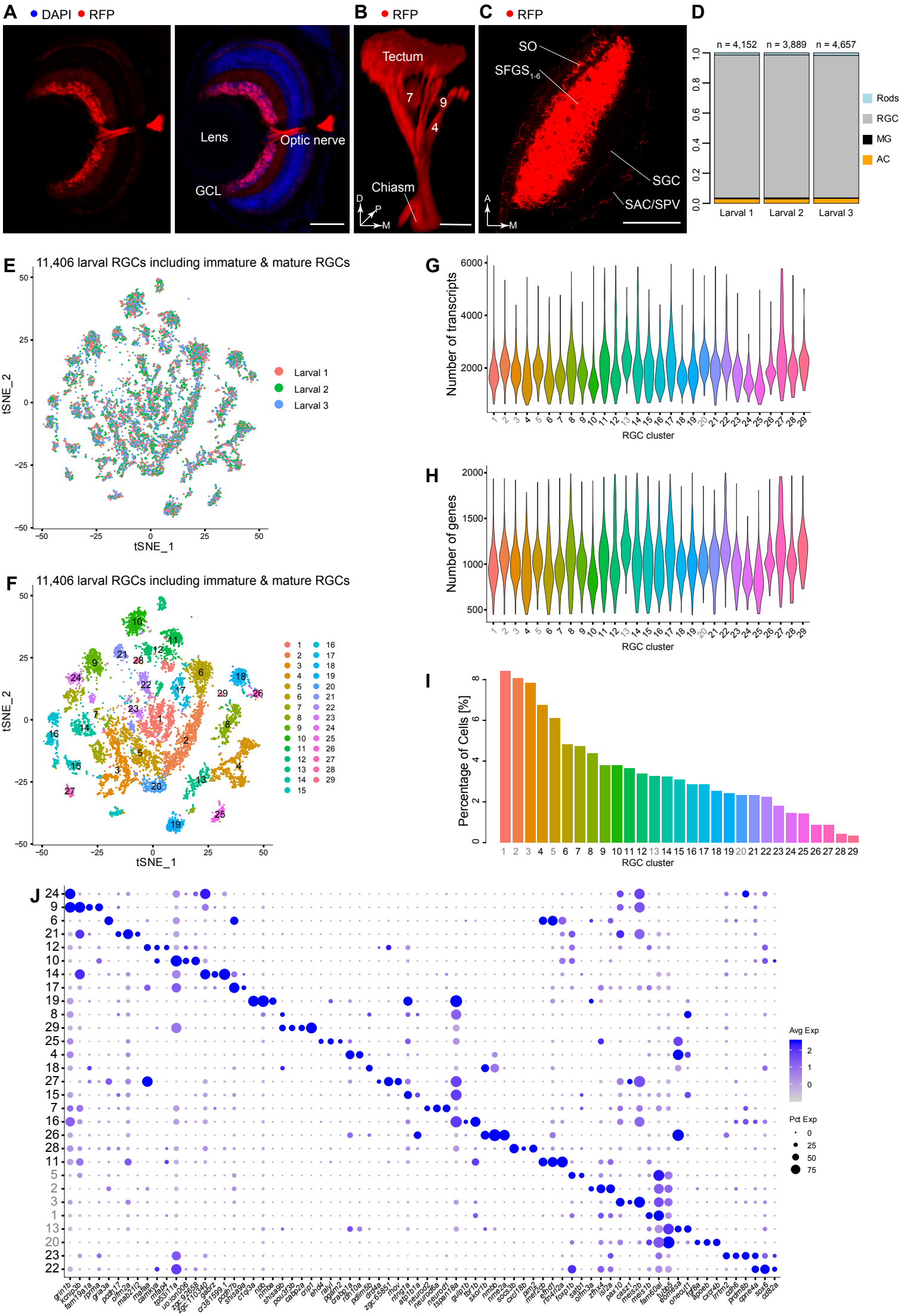
A
DAPI
RFP
Lens
Optic nerve
GCL
B
RFP
Tectum
7
9
4
Chiasm
C
RFP
SO
SFGS1-6
SGC
SAC/SPV
D
n = 4,152
n = 3,889
n = 4,657
Rods
RGC
MG
AC
Larval 1
Larval 2
Larval 3
E
11,406 larval RGCs including immature & mature RGCs
tSNE_1
tSNE_2
F
11,406 larval RGCs including immature & mature RGCs
G
Number of transcripts
RGC cluster
H
Number of genes
RGC cluster
I
Percentage of Cells [%]
RGC cluster
J
Avg Exp
Pct Exp

Figure S2. Molecular catalog of larval RGCs, related to Figure 3

(A) Immunohistochemical labeling of larval *Tg(isl2b:tagRFP)* retina sections show that RGCs, located in the innermost ganglion cell layer (GCL) of the retina, are robustly and uniformly labeled by RFP. Scale bar, 50 μm.

(B) 3D projection of RGC axons labeled in a live *Tg(isl2b:tagRFP)* larva. Anatomical locations corresponding to arborization fields (AF) 4, 7 and 9 and the tectum are marked. D, dorsal; P, posterior; M, medial. Scale bar, 50 μm.

(C) Confocal plane across retinotectal layers in a live *Tg(isl2b:tagRFP)* larva shows complete labeling of all innervation domains: SO, stratum opticum; SFGS, stratum fibrosum et griseum superficiale; SGC, stratum griseum centrale; SAC/SPV, stratum album centrale/stratum periventriculare. A, anterior; M, medial. Scale bar, 50 μm.

(D) Barplot showing relative proportions (y-axis) of RGCs and non-RGC contaminant classes in replicates of larval samples (x-axis). Cell numbers from each replicate are indicated on top.

(E) tSNE visualization of all larval RGC clusters combined with cells colored by sample of origin, showing lack of strong batch effects.

(F) tSNE visualization of 29 transcriptional clusters (colors) derived from 11,406 captured larval transcriptomes showing both immature and mature RGCs (points). Clusters are ordered in decreasing relative frequency.

(G) Violin plots showing the distribution of the number of transcripts detected per cell (y-axis) in each larval RGC cluster (x-axis).

(H) Violin plot showing the distribution of the number of genes detected per cell (y-axis) in each larval RGC cluster (x-axis).

(I) Relative frequency (y-axis) of larval RGC clusters (x-axis), ordered from highest to lowest.

(J) Dotplot showing the top three selectively enriched markers (columns) in each larval RGC cluster (rows). Representation and row ordering as in **Figure 3A**.

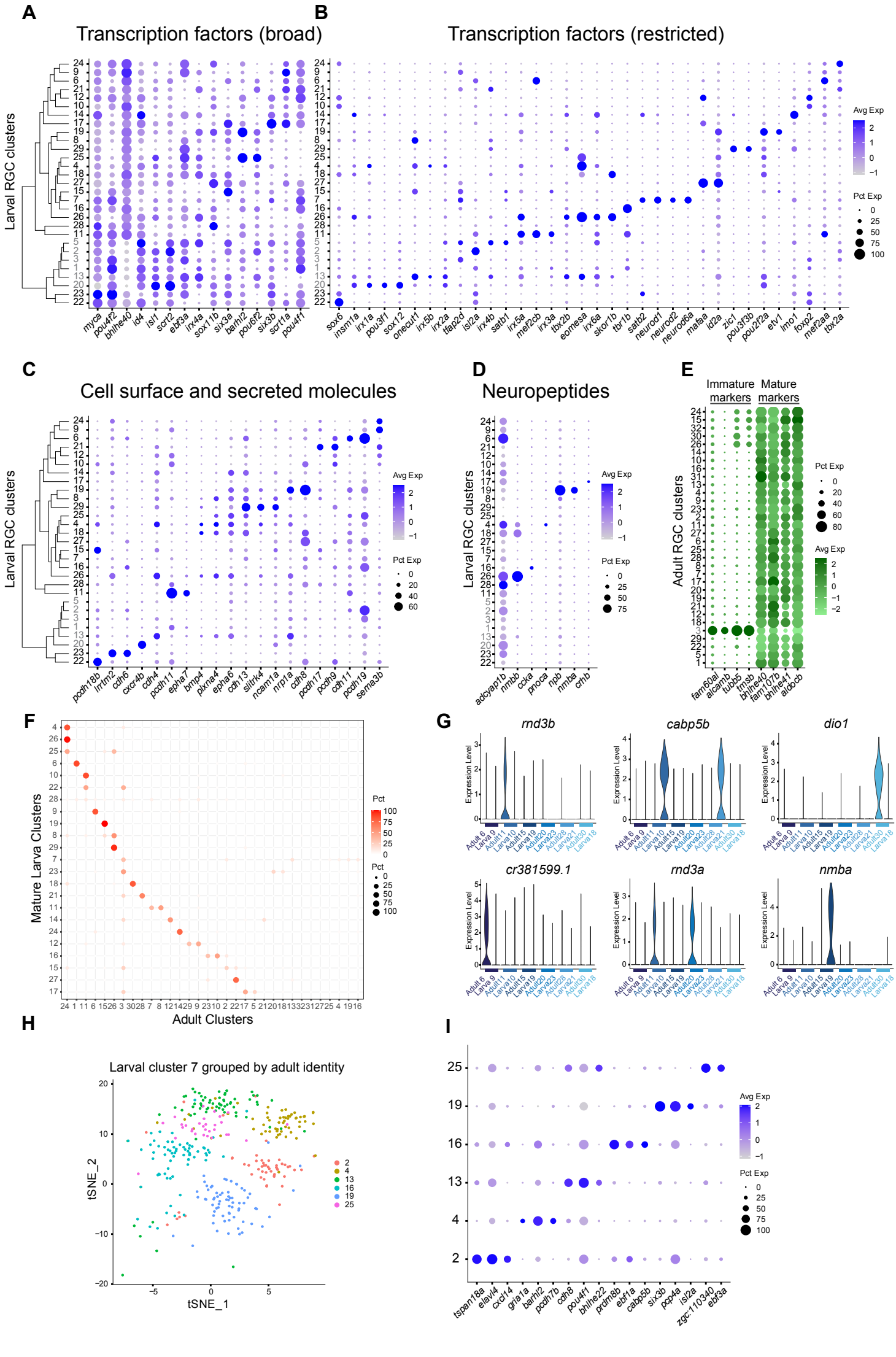
A
Transcription factors (broad)
B
Transcription factors (restricted)
Larval RGC clusters
myca pou4f2 bhlhe40 id4 isl1 scrt2 ebf3a irx4a sox11b six3a barhl2 pou6f2 six3b scrt1a pou4f1
sox6 insm1a irx1a pou3f1 sox12 onecut1 irx5b irx2a tfap2d isl2a irx4b satb1 irx5a mef2cb irx3a tbx2b eomesa irx6a skor1b tbr1b satb2 neurod1 neurod2 neurod6a mafaa id2a zic1 pou3f3b pou2f2a etv1 lmo1 foxp2 mef2aa tbx2a
Avg Exp
Pct Exp
C
Cell surface and secreted molecules
Larval RGC clusters
pcdh18b lrrtm2 cdh6 cxcr4b cdh4 pcdh11 epha7 bmp4 plxna4 epha6 cdh13 slitrk4 ncam1a nrp1a cdh8 pcdh17 pcdh9 cdh11 pcdh19 sema3b
D
Neuropeptides
Larval RGC clusters
adcyap1b nmbb ccka pnoca npb nmba cnb
E
Immature markers
Mature markers
Adult RGC clusters
fam60al alcam b tubb5 trnsb bhlhe40 fam107b bhlhe41 aldoc b
F
Mature Larva Clusters
Adult Clusters
Pct
G
rnd3b
cabp5b
dio1
cr381599.1
rnd3a
nmba
Expression Level
H
Larval cluster 7 grouped by adult identity
tSNE_1
tSNE_2
I
tspan18a elavl4 cxcl14 gria1a barhl2 pcdh7b cdh8 pou4f1 bhlhe22 prdm8b ebf1a cabp5b six3b pcp4a isl2a zgc:110340 ebf3a

Figure S3. Variably expressed genes across larval RGC types and maturational changes, related to Figure 3

(A-B) Dotplots highlighting variably expressed TFs in larval RGC clusters, subdivided into broad (A), and restricted (B) categories. Representation as in **Figure 3A**. The full list is provided in **Table S2**.

(C) Dotplot highlighting key cell surface and secreted molecules selectively expressed in larval RGC clusters.

(D) Dotplot highlighting neuropeptides selectively expressed in larval RGC clusters.

(E) Dotplot highlighting genes (columns) that distinguish immature versus mature larval RGC clusters (as in **Figure 3A**) across adult RGC clusters (rows), ordered as in **Figure 1G**.

(F) Transcriptional correspondence between adult and mature larval RGC clusters (as in **Figure 3D**) but transposed and renormalized to highlight the proportional mapping of each larval cluster (row) to adult clusters (columns). Circles and colors indicate the proportion of cells in a mature larval cluster (row) mapped to a corresponding adult RGC cluster (column) by the xgboost algorithm trained on adult RGCs. Each row is normalized to sum to 100%.

(G) Violin plots showing genes that are up- or down-regulated during maturation in a type-specific manner. Expression values (y-axis) of genes (panels) are plotted for each of the six 1:1 matching larval and adult clusters in panel D (columns). Colored bars indicate matching cluster pairs.

(H) tSNE visualization of larval cluster 7 cells (n = 539). Cells are grouped based on their adult identity as assigned by the supervised classifier.

(I) Dotplot highlighting differentially expressed genes between subclusters of larval cluster 7.

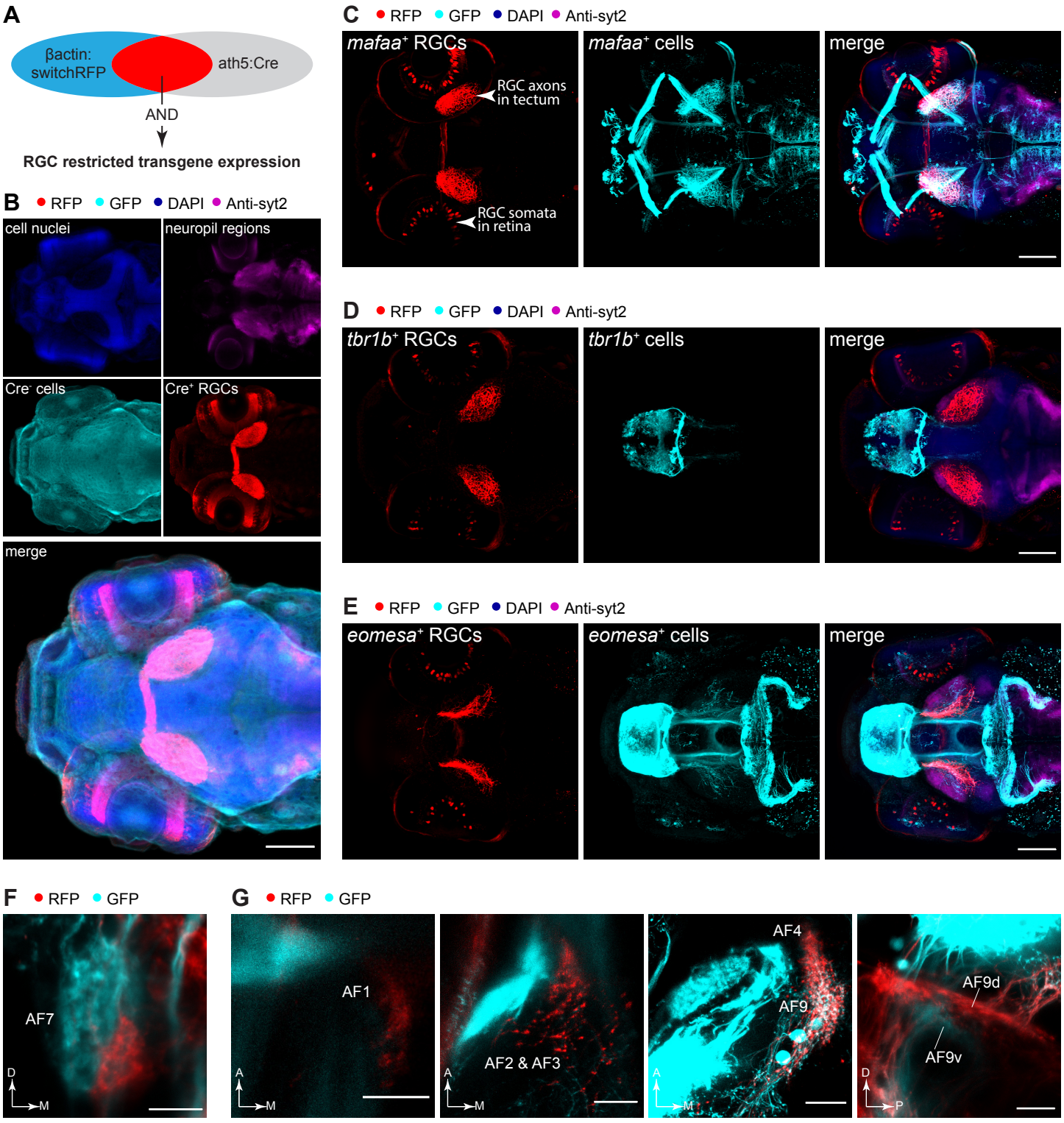
A
βactin: switchRFP
ath5:Cre
AND
RGC restricted transgene expression
B
RFP GFP DAPI Anti-syt2
cell nuclei
neuropil regions
Cre⁻ cells
Cre⁺ RGCs
merge
C
RFP GFP DAPI Anti-syt2
mafaa⁺ RGCs
RGC axons in tectum
RGC somata in retina
mafaa⁺ cells
merge
D
RFP GFP DAPI Anti-syt2
tbr1b⁺ RGCs
tbr1b⁺ cells
merge
E
RFP GFP DAPI Anti-syt2
eomesa⁺ RGCs
eomesa⁺ cells
merge
F
RFP GFP
AF7
D
M
G
RFP GFP
AF1
A
M
AF2 & AF3
A
M
AF4
AF9
A
M
AF9d
AF9v
D
P

Figure S4. Distinct anatomical features of molecularly defined RGC subclasses, related to Figure 4

(A) Genetic intersection via "AND" logic using the RGC-specific line *Tg(ath5:Cre)* refines transgene expression to RGCs in a ubiquitous driver line.

(B) Immunostained *Tg(ath5:Cre, ß-actin:loxP-GFP-loxP-tagRFP)* larvae show that Cre drives recombination specifically in RGCs as shown by GFP to RFP conversion. Cre^- cells continue to express the default reporter GFP. Scale bar, 100 µm.

(C-E) Characterization of novel RGC-cluster specific driver lines. Overview of immunostained *Tg(driver:QF2, QUAS:switchNTR, ath5:Cre)* larvae, where the "driver" corresponds to *mafaa* (C), *tbr1b* (D), and *eomesa* (E). Besides RFP-labeled cluster-specific RGCs, each marker is expressed in additional tissues: *mafaa* is expressed in muscles and neurons in midbrain and hindbrain, *tbr1b* is expressed in the forebrain and habenula, and *eomesa* is expressed in forebrain, habenula and cerebellum. Scale bar, 100µm.

(F) Frontal confocal view of AF7 innervated by $mafaa^+$ RGCs in the ventromedial neuropil as labeled in live *Tg(mafaa:QF2, QUAS:switchNTR, ath5Cre, isl2b:GFP)* larval fish. D, dorsal; M, medial. Scale bar, 10 µm.

(G) Confocal images of divergent extra-tectal $eomesa^+$ RGC innervations in AF1, AF2, AF3, AF4 and pretectal dorsal AF9 (AF9d) but not ventral AF9 (AF9v). A, anterior; M, medial; D, dorsal; P, posterior. Scale bar, 20 µm.

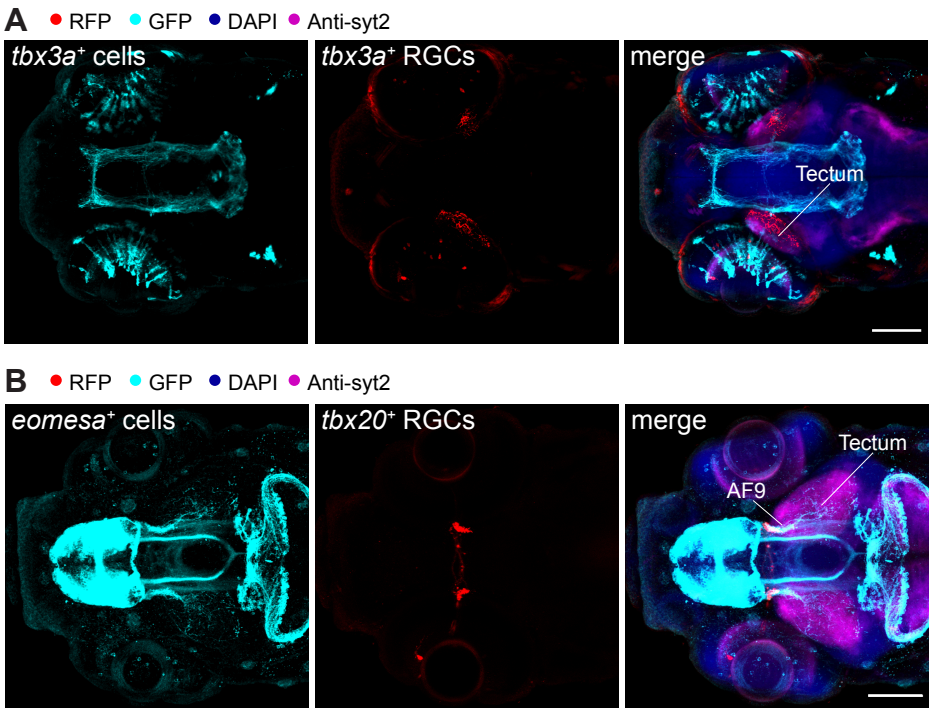
A
RFP
GFP
DAPI
Anti-syt2
tbx3a+ cells
tbx3a+ RGCs
merge
Tectum

B
RFP
GFP
DAPI
Anti-syt2
eomesa+ cells
tbx20+ RGCs
merge
Tectum
AF9

Figure S5. Unique morphotypes within RGC subclasses, Related to Figure 5

(A) Overview of immunostained *Tg(tbx3a:QF2, QUAS:switchNTR, ath5:Cre)* larvae. Besides RFP-labeled RGC types, *tbx3a* is expressed in other retinal cell types (Müller glia and bipolar cells) and hypothalamic neurons. Scale bar, 100 µm.

(B) Immunostained *Tg(eomesa:QF2, QUAS:GFP, tbx20:Gal4, UAS:NTR-mCherry)* larvae. Because there is no crosstalk between the binary expression systems Gal4-UAS and Q-system, *eomesa*$^{+}$ cells and *tbx20*$^{+}$ cells could be labeled independently and co-visualized in GFP and RFP, respectively. Scale bar, 100 µm.

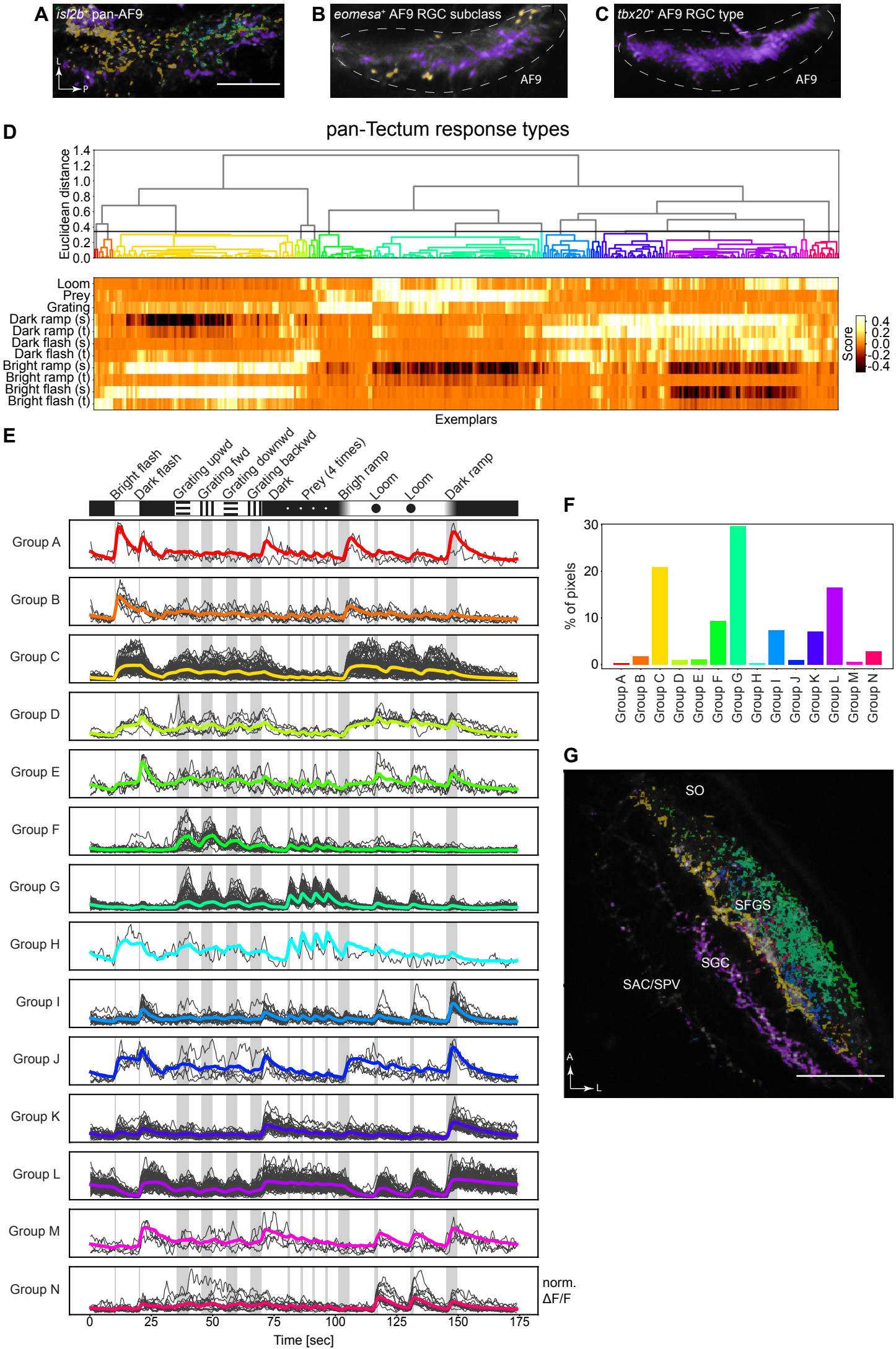
A
isl2b+ pan-AF9
L
P
B
eomesa+ AF9 RGC subclass
AF9
C
tbx20+ AF9 RGC type
AF9
D
pan-Tectum response types
Euclidean distance
1.4
1.2
1.0
0.8
0.6
0.4
0.2
0.0
Loom
Prey
Grating
Dark ramp (s)
Dark ramp (t)
Dark flash (s)
Dark flash (t)
Bright ramp (s)
Bright ramp (t)
Bright flash (s)
Bright flash (t)
Score
0.4
0.2
0.0
-0.2
-0.4
Exemplars
E
Bright flash
Dark flash
Grating upwd
Grating fwd
Grating downwd
Grating backwd
Dark
Prey (4 times)
Brigh ramp
Loom
Loom
Dark ramp
Group A
Group B
Group C
Group D
Group E
Group F
Group G
Group H
Group I
Group J
Group K
Group L
Group M
Group N
0
25
50
75
100
125
150
175
Time [sec]
norm.
ΔF/F
F
% of pixels
30
20
10
0
Group A
Group B
Group C
Group D
Group E
Group F
Group G
Group H
Group I
Group J
Group K
Group L
Group M
Group N
G
SO
SFGS
SGC
SAC/SPV
A
L

Figure S6. Distinct responses across retinotectal laminae, Related to Figure 6

(A-C) Representative recorded neuropil with pixels color-coded by response group assignment as determined in **Figure 6G-I** for *isl2b*$^{+}$ RGCs (A), *eomesa*$^{+}$ RGCs (B) and *tbx20*$^{+}$ RGCs (C). L, lateral; P, posterior. Scale bar, 20 µm.

(D) Fourteen main response groups can be distinguished from functional imaging across retinotectal laminae using *Tg(isl2b:Gal4, UAS:GCaMP6s)* larvae. Shown is the dendrogram from hierarchical clustering of response exemplars. Neuronal activity to a certain type of visual stimulus is indicated by the correlation score.

(E) Activity traces of fourteen classified tectal response groups shown in D aligned with the visual stimulus sequence. Shown are the average traces (colored) and all representing exemplars that fall into the group (grey).

(F) Quantification of relative frequency of *isl2b*$^{+}$ RGCs response groups in the tectum.

(G) Pixels originating from distinct RGC axons innervating tectal laminae were color coded by response group assignment. A, anterior; L, lateral. Scale bar, 50 µm.

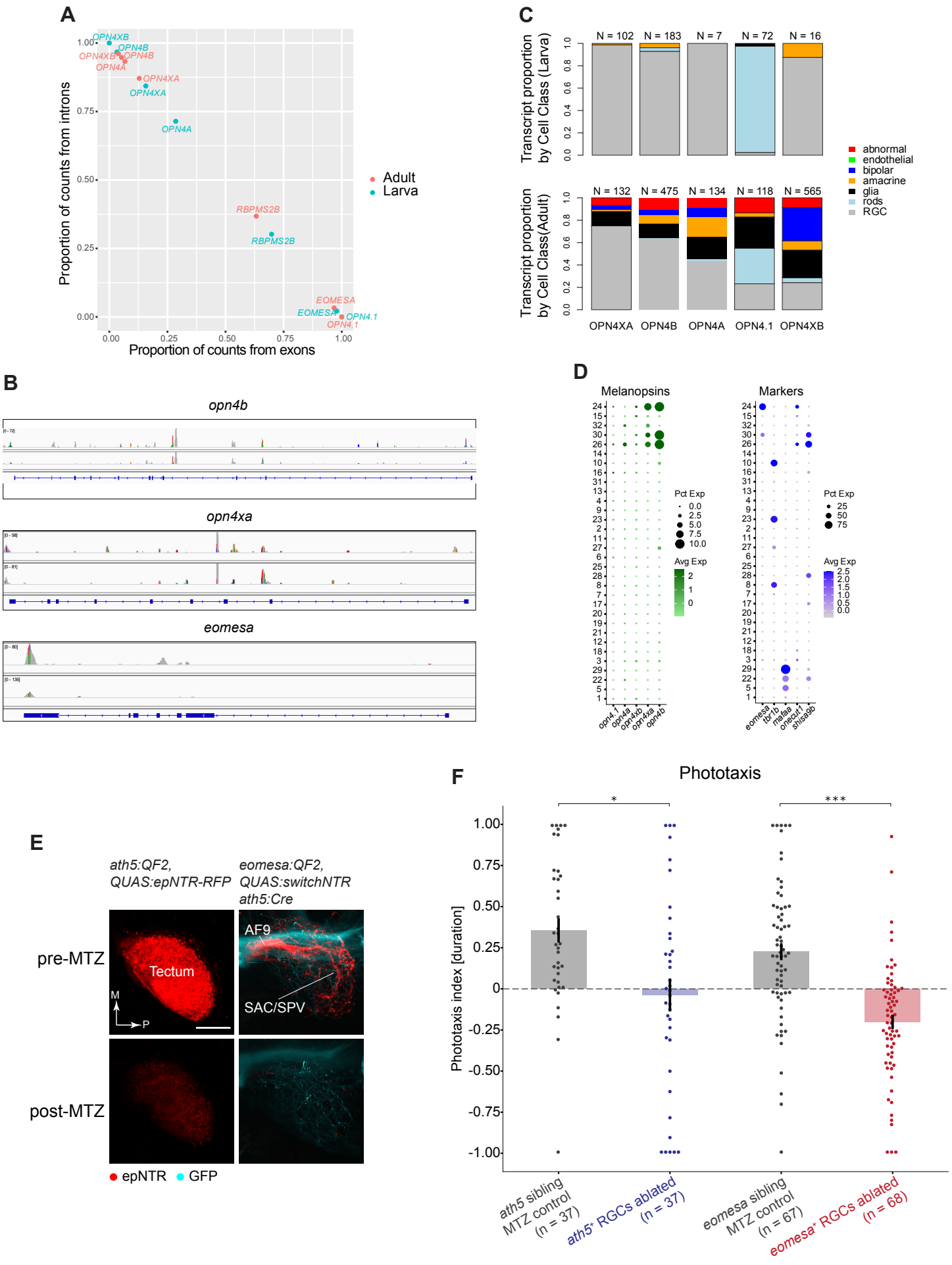
A
Proportion of counts from introns
Proportion of counts from exons
Adult
Larva
OPN4XB
OPN4B
OPN4XB
OPN4B
OPN4A
OPN4XA
OPN4XA
OPN4A
RBPMS2B
RBPMS2B
EOMESA
EOMESA
OPN4.1
OPN4.1
C
Transcript proportion by Cell Class (Larva)
Transcript proportion by Cell Class(Adult)
N = 102
N = 183
N = 7
N = 72
N = 16
N = 132
N = 475
N = 134
N = 118
N = 565
abnormal
endothelial
bipolar
amacrine
glia
rods
RGC
OPN4XA
OPN4B
OPN4A
OPN4.1
OPN4XB
B
opn4b
opn4xa
eomesa
D
Melanopsins
Markers
Pct Exp
Avg Exp
opn4.1
opn4a
opn4xb
opn4xa
opn4b
eomesa
tbr1b
mafaa
onecut1
shisa9b
E
ath5:QF2,
QUAS:epNTR-RFP
eomesa:QF2,
QUAS:switchNTR
ath5:Cre
pre-MTZ
post-MTZ
Tectum
AF9
SAC/SPV
M
P
epNTR
GFP
F
Phototaxis
Phototaxis index [duration]
ath5 sibling MTZ control (n = 37)
ath5+ RGCs ablated (n = 37)
eomesa sibling MTZ control (n = 67)
eomesa+ RGCs ablated (n = 68)

Figure S7. Intrinsic photosensitivity in the zebrafish retina and its implication in phototaxis, Related to Figure 7

(A) Relative proportions of intron (y-axis) and exon (x-axis) annotated transcripts for melanopsin genes, *eomesa,* and *rbpms2b* in the larval (blue) and adult (red) data. These counts were computed using velocyto (La Manno et al., 2018).

(B) Read alignment patterns at the loci corresponding to *opn4b* (*top*)*, opn4xa (middle)* and *eomesa (bottom)*. For each gene (panel), the gene body definition is provided in the bottom-most row, with exons denoted by boxes, introns by lines and the arrows indicating the 5' to 3' direction. The pile-up of read counts from two separate adult samples shown for each gene. While peaks for *eomesa* correspond to exonic locations, those for *opn4b* and *opn4a* are predominantly derived from introns, consistent with panel A.

(C) Barplots showing relative frequency (y-axis) of detection of transcripts of melanopsin genes (x-axis) in various cell classes in the larval (top) and adult (bottom) dataset. Cell classes, denoted by colors, correspond to those in **Figures S1A** and **S2D**, respectively. Recovered numbers of transcripts (intronic + exonic) are indicated on the top of each bar for each gene.

(D) Dotplots showing type-specific expression of melanopsin genes in adult RGCs, as in **Figure 7A.** *Left*: Of the five melanopsin homologs (columns), only *opn4xa* and *opn4b* have discernible expression in specific adult RGC clusters (rows) when intronic reads are accounted for. *Right: opn4xa* and *opn4b* expressing clusters include *eomesa*$^{+}$ RGC types but not *mafaa*$^{+}$ or *tbr1b*$^{+}$ types. C27, the only adult *eomesa*$^{-}$ RGC type that expresses melanopsin, is marked by the co-expression of *onecut1* and *shisa9b*.

(E) Maximum projections of the tectum of live imaged transgenic fish expressing nitroreductase (NTR) in *ath5*$^{+}$ RGCs (left) and *eomesa*$^{+}$ RGCs (right) before and after treatment with metronidazole (MTZ). M, medial; P, posterior. Scale bar, 50 μm.

(F) Phototaxis index (PI) values as determined by time spent (duration) in the dim or lit half of the arena for all tested groups: NTR^{-} *Tg(ath5:QF2)* and *Tg(eomesa:QF2)* control siblings as well as *ath5*$^{+}$ RGC-ablated blind fish and *eomesa*$^{+}$ RGC-ablated larvae. Shown is a barplot with a superimposed dotplot, where each dot represents one fish. Error bars represent SEM. * $p<0.05$, *** $p<0.001$ (Dunn post-hoc test).